



ELSEVIER

Contents lists available at ScienceDirect

Comptes Rendus Geoscience

www.sciencedirect.com



Hydrology, Environment

Purus River suspended sediment variability and contributions to the Amazon River from satellite data (2000–2015)



Andre Luis Martinelli Real dos Santos ^{a,b,*}, Jean Michel Martinez ^c,
Naziano Pantoja Filizola Jr. ^{b,d}, Elisa Armijos ^{b,e}, Luna Gripp Simões Alves ^a

^a Brazilian Geological Service (CPRM), Manaus, AM, Brazil^b H2A Research Group, UFAM, Manaus, AM, Brazil^c Institut de recherche pour l'environnement (IRD), Brasília, DF, Brazil^d Universidade Federal do Amazonas, Manaus, AM, Brazil^e CLIAMB–Instituto Nacional de Pesquisas da Amazônia UEA, Manaus, AM, Brazil

ARTICLE INFO

Article history:

Received 8 June 2016

Accepted after revision 11 May 2017

Available online 31 July 2017

Handled by François Chabaux

Keywords:

Amazon

Purus

Remote Sensing

Suspended Sediments

Hydrology

ABSTRACT

The Purus River is one of the major tributaries of Solimões River in Brazil, draining an area of 370,091 km² and stretching over 2765 km. Unlike those of the other main tributaries of the Amazon River, the Purus River's sediment discharge is poorly characterized. In this study, as an alternative to the logistic difficulties and considering high monitoring costs, we report an experiment where field measurement data and 2700 satellite (MODIS) images are combined to retrieve both seasonal and interannual dynamics in terms of the Purus river sediment discharge near its confluence with the Solimões River. Field radiometric and hydrologic measurements were acquired during 18 sampling trips, including 115 surface water samples and 61 river discharge measurements. Remote sensing reflectance gave important results in the red and infrared levels. They were very well correlated with suspended sediment concentration. The values of R^2 are greater than 0.8 (red band) and 0.9 (NIR band). A retrieval algorithm based on the reflectance in both the red and the infrared was calibrated using the water samples collected for the determination of the surface-suspended sediment concentration (SSS). The algorithm was used to calculate 16 years of SSS time series with MODIS images at the Purus River near its confluence with the Solimões River. Results from satellite data correlated with *in situ* SSS values validate the use of satellite data to be used as a tool to monitor SSS in the Purus River. We evidenced a very short and intense sediment discharge pulse with 55% of the annual sediment budget discharged during the months of January and February. Using river discharge records, we calculated the mean annual sediment discharge of the Purus River at about of 17 Mt·yr⁻¹.

© 2017 Académie des sciences. Published by Elsevier Masson SAS. All rights reserved.

* Corresponding author. Brazilian Geological Service (CPRM), Manaus, AM, Brazil.

E-mail addresses: andre.santos@cprm.gov.br (A. Santos), martinez@ird.fr (J.M. Martinez), naziano.filizola@gmail.com (N.P. Filizola Jr.), armijos.elisa@gmail.com (E. Armijos), luna.alves@cprm.gov.br (L.G.S. Alves).

1. Introduction

Every year, the oceans receive approximately 20 billion tons of suspended sediments because of erosion and transportation through river systems (Allen, 2008). Tropical basins are the largest suppliers of that amount. The Amazon River's sediment discharge has been estimated at

between 800 and 1200 Mt·yr⁻¹ (Filizola et al., 2011; Guyot et al., 2005; Meade et al., 1985), with the Andean region being the main source of suspended sediments (Filizola and Guyot, 2009, 2011; Gibbs, 1967; Latrubesse et al., 2005).

The Purus River (Fig. 1A) is one of the major tributaries of the Solimões River, with an average annual water discharge (Q) of 10,700 m³ s⁻¹ (Filizola and Guyot, 2009). The high-water period usually extends from April to May, while the low-water period usually occurs from October to November (Fig. 1B). The erosive process acting in the river basin moves sediments deposited in the Andean forestland. This region had been experiencing an uplift of the basement by tectonic action (Espurt et al., 2007), favoring a greater supply of sedimentary material to be transported by the Amazon River and its tributaries that have their headwaters at this region. This is the case of the Purus and Juruá Rivers, for example. Recent data on SSS indicate significant longitudinal variability in those rivers (Filizola and Guyot, 2009). The Purus basin extends over 370,091 km² (Melo, 2012) and its sediment discharge was reported as 47.2 Mt·yr⁻¹ (Filizola et al., 2011). However, the Brazilian Ministry of the Environment (<http://www.mma.gov.br>) has put this basin on alert due to the rapid land-use changes resulting from increasing illegal logging, which may drastically alter sediment production and transportation. To monitor these changes, the Brazilian National Water Agency (ANA) conducts quarterly water sampling at key stations, but that frequency is not enough to

assessing seasonal and interannual dynamics of the river sediment discharge.

Monitoring of suspended sediment in large rivers, such as those at the Amazon basin, is time-consuming, and its accuracy is generally limited by operating costs and local infrastructure. This makes it difficult to collect frequent SSS samples. More recently, indirect techniques, especially those using satellite images, have been proven to supplement conventional sampling techniques efficiently in large rivers. These methods, which have been tested since the early 21st century, are less expensive and less time-consuming (Filizola et al., 2011; Martinez et al., 2009). Remote sensing techniques were first applied to hydro-sediment data assessment several decades ago in the Amazon Basin (Bradley et al., 1979; Mertes et al., 1993), but the use of satellite images for sediment flux monitoring is far more recent (Espinoza Villar et al., 2012; Martinez et al., 2009).

This new method offers enhanced spatial and temporal resolutions compared to conventional water sampling practices based on field gauging stations, particularly in poorly gauged basins for large rivers. Using the Moderate Resolution Imaging Spectroradiometer (MODIS) image time series, Martinez et al. (2009) demonstrated the possibility of assessing the evolution of river sediment discharge from space over the Amazon River. Similarly, Park and Latrubesse (2015) by MODIS images have investigated water-mixing processes at the confluence of the Negro River and of the Solimões River. Adding field spectroradiometry data to the calibration of the reflectance

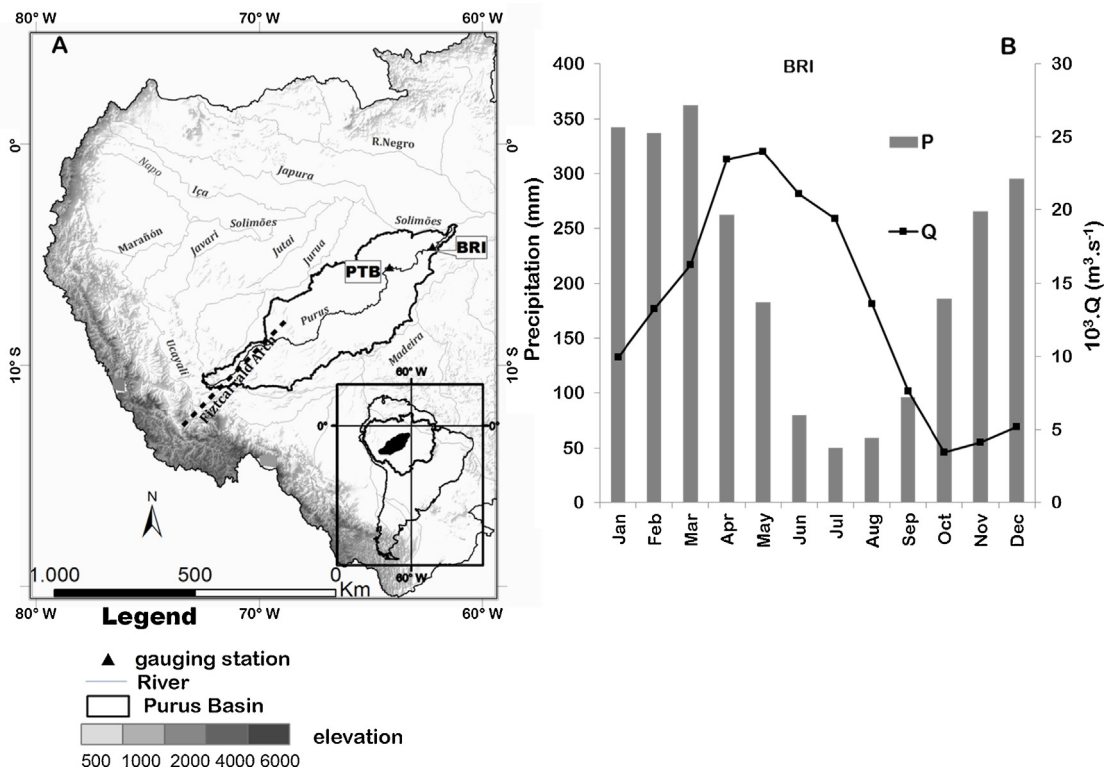


Fig. 1. A. Location of the Purus River catchment. B. Average water discharge at the Beruri gauging station (2009–2014) and mean rainfall over the catchment as retrieved by TRMM (2001–2014).

extracted from MODIS images, Espinoza et al. (2012) presented suspended sediment transport processes along the Madeira River.

This study provides the first assessment of Purus sediment discharge over 16 years, using a large field measurement database that includes river water discharge measurements, water samples and field radiometric measurement acquired over two hydrological years.

2. Materials and methods

2.1. Study area

The Purus River Basin has an altitudinal gradient from 420 masl to 28 masl, with an average slope of 1.24% (Melo, 2012). Average precipitation in the basin, calculated using the Tropical Rainfall Measuring Mission (TRMM) data set from 2001 to 2014, was about 2300 mm·yr⁻¹. The wet season occurs from January to March and the dry season usually occurs from June to August. Based on quarterly measurements, Filizola et al. (2009) found an average suspended sediment concentration of 19 mg·L⁻¹.

Two gauging stations installed on the Purus River are considered in this study, Beruri (BRI) and Paricatuba (PTB). They are located at 30 km and 120 km, respectively, upstream from its confluence with the Solimões River. These gauging stations are influenced by the backwater-effect from the Solimões especially during the months of April until August (Fig. 1A) and are monitored by ANA and the Brazilian Geological Service (CPRM).

2.2. Data collection and processing

Water discharge (Q) was measured using an Acoustic Doppler Current Profiler (ADCP Rio Grande 600 kHz) coupled with a differential GPS with less than 3% of accuracy. The daily discharge is calculated from the stage–discharge relationship.

Water samples were collected at the river's surface using 2-L sampling bottles from 2010 to 2015 at the PTB and BRI gauging stations. For sampling suspended sediments in a cross section, a discrete water sampler of 5 L tied to a 50-kg weight was used. The cross section was divided in two or three profiles (25%, 50% and 75%) and at each profile four to five points were sampled. The protocol of the sampler and laboratory processes is the one recommended by the Observatory HYBAM (www.ore.hybam.com). In this protocol, using a pre-weight filter, the total volume of water samples was filtered through a 0.45- μ m acetate cellulose filter passing through an oven at 105 °C for 2 h (ASTM, 2003) and reweighed. The average sediment concentration at the cross section is obtained by weighting the discharge.

The particle size in the surface and cross-section samples was determined through the Malvern Mastersizer 2000 laser granulometer at the CPRM laboratory, in Manaus. We took samples at different periods of the hydrologic regime.

There is a relationship between SSS and total suspended sediments (TSS). The transformation from SSS to the TSS, at

each cross section, was established at specific seasons of the year using the same procedure established by Filizola (2003) with the ORE-HYBAM field campaigns done during the 1990s.

Remote sensing reflectance measurements (Rrs) were made following the Mobley (1999) protocol, simultaneously measuring irradiance and radiance with TriOs RAMSES hyperspectral radiometers. To obtain reflectance, three spectral radiometers (model TriOs RAMSES) were placed outside the water in a particular spatial geometric arrangement. One sensor was positioned at 40° off-nadir to measure direct upward radiance (L_u). The second sensor was positioned at 40° from the zenith to measure downward radiance (L_d). The irradiance (E_d) sensor was vertically positioned at 90°, as suggested by Martinez et al. (2015). Equation (1) was used to calculate field reflectance (Rrs):

$$Rrs = \frac{L_u - f \times L_d}{E_d}; \quad (1)$$

where f depends on the shear of the water surface, and is 0.028 when the wind speed is less than 5 m·s⁻¹ (Mobley, 1999) as in the case of the study area. To compare the “in situ” radiometric data with satellite data, only radiation in the red (Band: 1620–670 nm) and near infrared (Band: 2841–876 nm) range were extracted. Those values were calculated by taking the average of all data in each range.

The MODIS images were obtained from NASA database using GETMODIS software, which can import the images of interest from a selected area. The MOD3R algorithm (<http://www.ore-hybam.org/index.php/eng/Software/Getmodis-Mod3r>) was used to extract River Water Reflectance from the MOD09 (TERRA satellite) and MYD09 (AQUA satellite) products. That algorithm classifies each pixel in four categories, 0 = total cloud cover, 1 = insignificant cloud noise, 2 = caution to use data and 3 = insufficient data acquisition. This study used the indices 1 and 2. The images used were a result of an 8-day composite and mixed observation. Both have two types of spatial resolution, A1 (500 m) and Q1 (250 m). We analyzed MODIS time series products using MOD09 and MYD09 surface reflectance with 250 m (red and near infrared).

To calculate the flux of surface-suspended sediments (Q_s), the method proposed by Vanoni (1977) was used. This means: $Q_s = TSS \times Q \times 0.0864$, where TSS is obtained by MODIS images data every eight days and Q corresponds to the discharge obtained on the same day as the SSS samples.

3. Results and discussion

3.1. Water discharge

Table 1 summarizes the data obtained during the 42 field measuring campaigns, in which 61 discharge measurements were obtained during years 2013–2015 at Purus River. During this period, the average discharge at PTB was 10,300 m³·s⁻¹. This value is very close to the 10,700 m³·s⁻¹ reported by Filizola and Guyot (2009). The maximum discharge registered was 17,000 m³·s⁻¹ (April

Table 1

Summary of the SSS concentration and Discharge (Q) measurements assessed at BRI and PTB stations during 42 field-sampling trips.

Station	Period	# SSS samples	SSS (mg·L ⁻¹)			# Q samples	Q (10 ³ m ³ ·s ⁻¹)		
			Min	Ave	Max		Min	Ave	Max
BRI	10 Jun. to 15 Feb.	82	3	43	322	42	2.3	13.1	24.9
PTB	13 Apr. to 15 Feb.	33	4	49	390	19	3.6	10.3	16.9

2014) and the minimum was about 3600 m³·s⁻¹ (October 2013). At the BRI station, the average discharge was measured at 13,100 m³·s⁻¹. The maximum registered discharge was about 24,900 m³·s⁻¹ (May–June), and the minimum was 2300 m³·s⁻¹ (October–November). The maximum discharge difference between these two stations is a result of the backwater effect (Meade et al., 1979), and can be better evidenced at BRI (downstream), with an increase of 27% of the discharge with respect to PTB, located about 90 km upstream of BRI.

3.2. Suspended sediments

The average value about SSS from the 115 surface water samples at PTB was about 49 mg·L⁻¹. The maximum value was 390 mg·L⁻¹ for January 2015 and 4 mg·L⁻¹ was the minimum registered in June 2013. At BRI, the mean SSS was 43 mg·L⁻¹, the maximum: was 322 mg·L⁻¹ in January 2015 and the minimum was 3 mg·L⁻¹ in June 2013. These values show a seasonal variability at the Purus River by about two orders of magnitude. The high variability of SSS on the Purus River turns the characteristic from those of black water (SSS < 20 mg·L⁻¹) into those of white water (larger than 100 mg·L⁻¹, Sioli (1984)). However, we also observed that between the two gauging stations PTB and BRI, there is a compartment differential due to the influence of the Solimões River, which supplies the suspended sediments at BRI where there is a major influence.

The result of granulometry to suspended sediments in the Purus River is composed by clay and silt particles (10–30 μm), but in January and February we observed a finer type (1–4 μm). The size distributions are observed both on the surface and in the cross section; therefore, with

a surface sample, it is possible to know the value of the suspended sediments in cross section.

The good relationship between SSS and TSS ($R^2 = 0.97$) permits to calculate the suspended sediments flux during this period (Fig. 2); consequently, the surface samples is representative of the samples taken at the cross section. It was possible to calculate the QS of 17 Mt·yr⁻¹, value close to that obtained by Filizola and Guyot (2009), using one measure by month of TSS and de Q from Beruri station. This, represents almost 2% of the total QS of the Solimões River (Espinoza et al., 2017, this issue).

3.3. Radiometric measurements

Table 2 presents the maximum and minimum reflectance values obtained from MODIS data and Field Reflectance Measurements (FRM) over the 2000–2015 period. For BRI, reflectance values ranged from 0.017 to 0.238 on the red band in MODIS images and from 0.018 to 0.279 in FRM. On the near-infrared band, reflectance values were between 0.007 and 0.132 in MODIS images and between 0.002 and 0.126 in FRM. The same order of magnitude was observed for PTB and between the values obtained by satellite and by FRM. This suggests that using satellite data to estimate field reflectance is admissible.

Field radiometric measurements were used to develop a SSS concentration retrieval algorithm and to assess the accuracy of the MODIS reflectance over river channels. Fig. 3 reveals the relationship between FRM and MODIS reflectance retrieved using MOD3R software from 8-day composites acquired over the same period and the same location. MODIS reflectance in red band shows fine agreement with field measurements and low bias, of 8%,

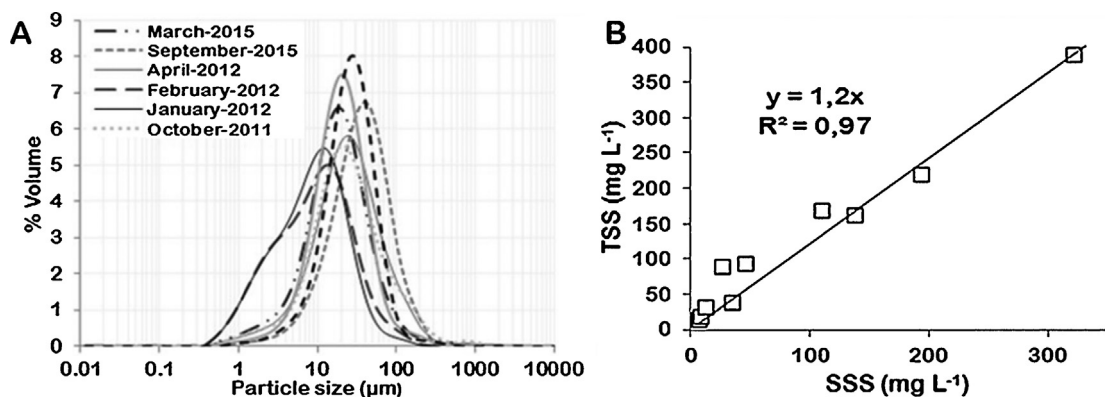


Fig. 2. A. Particle size in Purus River at Beruri gauging station. B. Relationship between total suspended sediments (TSS) and surface-suspended sediment (SSS).

Table 2
Results of MODIS and FRM reflectance measurements for BRI and PTB.

Station	Period	# MODIS samples	# FRM samples	MODIS				FRM			
				R		NIR		R		NIR	
				Min	Max	Min	Max	Min	Max	Min	Max
BRI	10 Jun. to 15 Feb.	42	17	0.017	0.238	0.007	0.132	0.018	0.279	0.002	0.126
PTB	13 Apr. to 15 Feb.	19	14	0.028	0.225	0.017	0.108	0.026	0.285	0.004	0.139

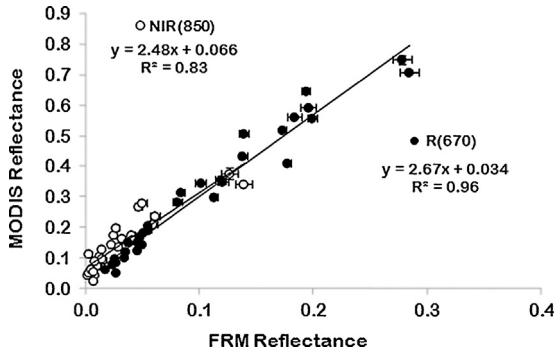


Fig. 3. Comparison between field radiometric measurements (FRM) and MODIS satellite reflectance (MOD/MYD09Q1 products) at red (R) and infrared (NIR) channels, acquired during field measurements.

confirming the efficiency of the MODIS products to deliver fine radiometric data. In the infrared, MODIS reflectance is close to the field measurements, although for the low range the satellite data overestimate reflectance. The overall results indicate that satellite data could be used as an estimator for field reflectance measurement. For the error-bars associated with field reflectance, only the standard deviation between the means of the reflectance values in each sample contained in the intervals of the bands 1 and 2 was considered. For the reflectance from MODIS images, the main sources of uncertainty are pixel size, atmospheric noise, adjacency of distinctive features (soil, forest and water) in the same pixel and the angle of sensor view. The surface reflectance values of the MODIS products are sized to 10^4 and then converted into 16-bit integers. Therefore, only after applying these factors in field reflectance ($10^4 \pi$), it is possible to compare these data with those of MODIS reflectance.

Fig. 4 shows the variation of FRM as a function of SSS concentration for the red (A) and infrared channels (B). In the red band, reflectance is linearly correlated with SSS concentration for low values in the 0–100 $\text{mg}\cdot\text{L}^{-1}$ range. For higher concentration, reflectance shows non-linear behavior, although the lack of concentration in the [100–300] range makes it difficult to fully assess the relationship. In the infrared, reflectance varies quasi-linearly with concentration, but there is a significant dispersion at lower concentration.

Based on these observations, we set up a retrieval model based on the red and infrared bands. The red channel is used to retrieve the low concentration range, while the infrared channel is used to retrieve the higher range. The model used for SSS estimation was therefore based on red reflectance when these values were lower than 0.06 and on near-infrared reflectance for higher values. The lack of reflectance data between 0.07 and 0.08 values, prevented us to determine with more accuracy the breakpoint arbitrary. When the concentration increases but does not change the reflectance values, is the saturation limit for the red band.

3.4. Purus River sediment discharge retrieval

The two-band retrieval model is used to process the MODIS reflectance time series, making it possible to derive a 16-year SSS record. **Fig. 5** compares the SSS time series at the BRI station (2000–2015) retrieved from MODIS images and the SSS measurements acquired during the field sampling trips.

Satellite makes it possible to retrieve the seasonal dynamic of the SSS concentration with unprecedented detail, showing that the Purus River exhibits a very short and intense sediment pulse occurring each year usually between December and February. Over the period of observation, SSS interannual records do not show any

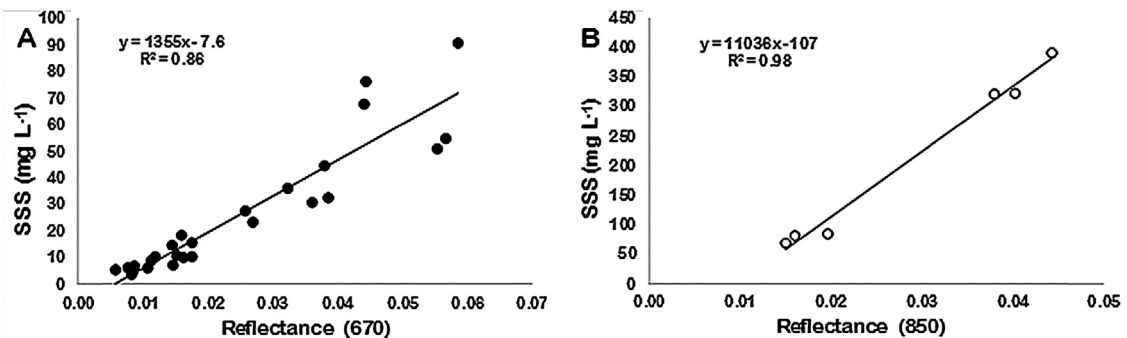


Fig. 4. Relationship between water sample SSS data and FRM reflectance data. A (red band 1670 cm^{-1}) and B (NIR band 2850 cm^{-1}).

significant change in trend. Satellite-retrieved and field SSS estimates are exceptionally well correlated for most of the hydrological cycle, with a mean RMSE of 40%.

During peak sediment discharge, some stronger discrepancies appear between satellite-derived SSS estimates and field measurement, for example as in January, which may be caused by the time delay between the samples and the satellite images of good quality, because they hardly match the very-day of sampling, in particular during the rainy season. The satellite data used contains the best possible daily observation within the 8-day period. The criteria settled down for the selection of satellite data was the lowest viewing angle, the absence of clouds or cloud shadows and the lowest aerosol load.

Several authors have shown that suspended sediment is not correlated with discharge in the Amazon River because the sediment discharge comes almost exclusively from the Andes, although the river receives significant inputs from clear/black waters located in the plain, introducing downstream a hysteresis between TSS concentration and discharge relationship. Our results demonstrate the same partial decorrelation between sediment discharge and river discharge for the Purus River, but with a large time lag (three to four months) than for the Amazon main stem at Óbidos (two to three months, [Filizola, 2003](#); [Filizola et al., 2011](#); [Martinez et al., 2009](#)).

We estimate the Purus River sediment discharge from TSS concentration records and water discharge time series at the BRI station. [Fig. 6](#) displays the monthly average

sediment discharge at the BRI station assessed over the 2000–2015 period. Sediment discharge varied from 6200 t·day⁻¹ in August up to 200,476 t·day⁻¹ in January.

Our results demonstrate that the solid discharge pattern of the Purus River is significantly different from that of other major Amazonian rivers, such as the Madeira River or the Amazon River ([Guyot et al., 2005](#), [Martinez et al., 2009](#)). The peak of TSS occur during a short time (approximately 10 days) between the months of December and January, while in the other rivers cited the peaks have a longer duration, around 2 or even 3 months. The backwater effect and the lateral inputs from the Solimões River delay and alter the Purus River flood pattern and may contribute to the observed important time lag between sediment discharge and river discharge at the Purus River confluence. Another important feature is the strength of the sediment discharge peak of the Purus River in relation to other Amazonian rivers. The months of January and February account for 55% of the annual sediment budget of the Purus River. For the Amazon River, half the annual sediment budget (i.e. 51%) is discharged from January to April ([Filizola et al., 2011](#); [Martinez et al., 2009](#)). For this same four-month period, January–April, the Purus River's discharge accounts for 72% of its annual sediment budget.

Based on our results, we assess an average annual sediment discharge of 17 Mt·yr⁻¹, representing 2% of total suspended sediments flux in the Solimões River ([Espinoza et al., 2017](#), this thematic issue). This value is almost 31% lower than the estimates made by [Filizola and Guyot](#)

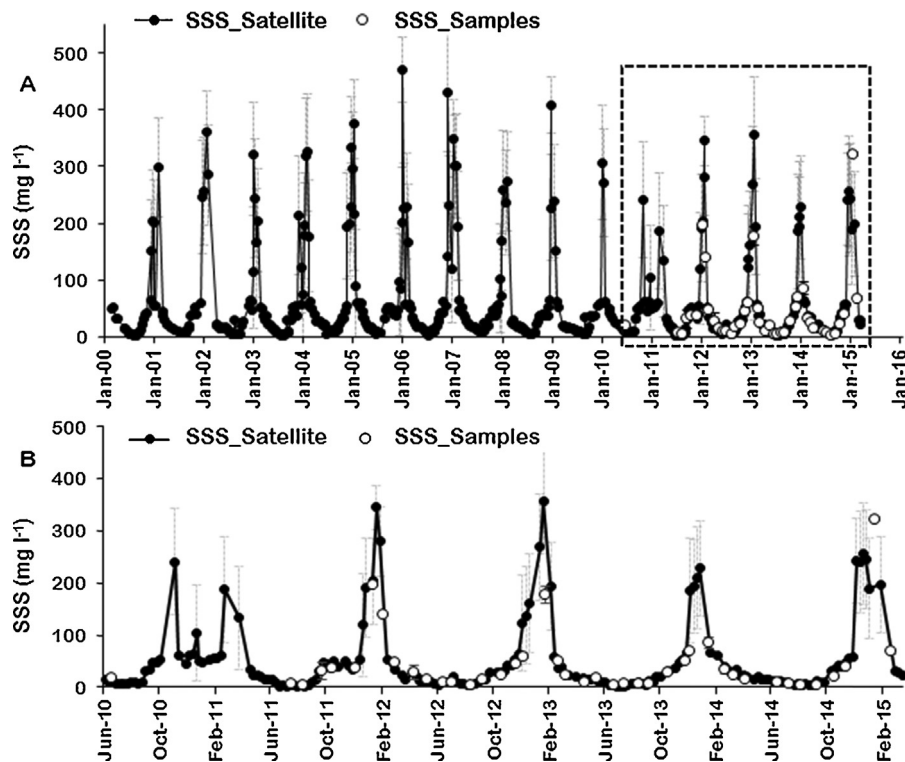


Fig. 5. A. Surface Suspended Sediment data set obtained from satellite (2000–2015). B. Details about the period used for validation with “in situ” suspended sediment data. Vertical grey bars are deviation from pixel feature adjacencies.

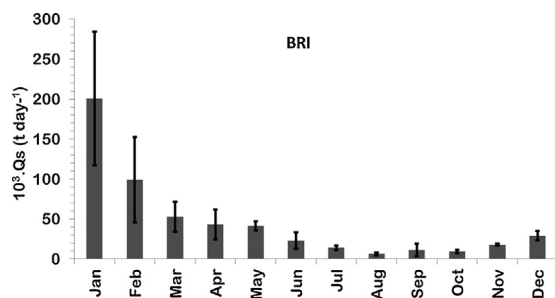


Fig. 6. Average monthly solid discharge based on liquid discharge measurements (2009–2014 period) and SSS based on MODIS images for the same period. Vertical black bars are standard deviation from solid discharge each month.

(2009), but these authors made use of a relatively small number of quarterly measurements by ANA (i.e. 51 samples), which is much less significant than the number of estimates used in this present work. We also assessed a specific suspended sediment yield for the whole Purus catchment of $46 \text{ t}\cdot\text{km}^{-2}\cdot\text{yr}^{-1}$, a value in the range of the yield assessed for most catchments draining the Brazilian shield in the Amazon River Basin. So, satellite data made it possible to calculate the suspended sediment flux, but with a greater frequency and with less logistic costs.

4. Conclusions

This study represents the most complete work produced about the Purus River sediment discharge variability at both long-term and seasonal scales. Using an important field database including radiometric and hydrologic measurements, we assessed a retrieval algorithm making it possible to derive SSS concentration time series from space. We analyzed a 16-year SSS concentration time series calculated from MODIS images over the Purus River confluence with the Solimões River. The Purus River sediment discharge peak showed a very intense pattern with more than half of the sediment budget being delivered in two months. Future works will consider the analysis of sediment patterns in areas located more upstream in order to limit the influence of the Solimões River backwater effect on the Purus River. The identification of the erosion zones in the catchment will be mapped in order to better understand the temporal dynamics of the suspended sediment on the river, particularly in relation to land-use changes such as deforestation.

References

Allen, P.A., 2008. Time scales of tectonic landscapes and their sediment routing systems. *Geol. Soc. Lond. Spec. Publ.* 296 (1), 7–28.
 ASTM, 2003. Standard test method for dynamic young's modulus, shear modulus and poisson's ratio by impulse excitation of vibration. ASTM International, West Conshohocken 1876–1878.

Bradley, J., Eden, M.J., Rice-Evans, P., 1979. Remote sensing of suspended sediment in Amazonian rivers from Landsat imagery. In: Allen, J.A., Harris, R. (Eds.), *Remote sensing and national mapping, the Remote Sensing Society*. University of Reading, Reading, UK, pp. 110–116.
 Espinoza, R., Martinez, J.M., Armijos, E., Espinoza, J.C., Filizola, N., dos Santos, A., Willems, B., Fraizy, P., Santini, W., Vauchel, P., 2017. Spatio-temporal monitoring of suspended sediment in the Solimões River 2000–2014. *C. R. Geoscience* 349 (this issue).
 Espinoza, R., Martinez, J., Guyot, J.G., Fraizy, P., Armijos, E., Crave, A., Bazán, H., Vauchel, P., Lavado, W., 2012. The integration of field measurements and satellite observations to determine river solid loads in poorly monitored basins. *J. Hydrol.* 444–445, 221–228.
 Espinoza Villar, R., Martinez, J.M., Texier, M., Guyot, J.G., Fraizy, P., Menezes, P., Oliveira, E., 2012. A study of sediment transport in the Madeira River, Brazil, using MODIS remote-sensing images. *J. S. Am. Earth Sci.* 1–10, 4–9.
 Espurt, N., Baby, P., Brusset, S., Roddaz, M., Hermoza, W., Regard, V., Antonie, P.-O., Salas-Gismondi, R., Bolaños, R., 2007. How does the Nazca Ridge subduction influence the modern Amazonian foreland basin? *Geology* 35 (6), 515–518.
 Filizola, N., 2003. *Transfert sédimentaire actuel par les fleuves amazoniens (Thèse)*. Université Toulouse-3–Paul-Sabatier, Toulouse, France (273 p.).
 Filizola, N., Guyot, J.-L., 2009. Suspended Sediment Yield in the Amazon Basin: an assessment using Brazilian national data set. *Hydrol. Processes* 23 (22), 3207–3215. <http://dx.doi.org/10.1002/Hyp.7394>.
 Filizola, N., Guyot, J.-L., 2011. Fluxo de sedimentos em suspensão nos Rios da Amazônia. *Rev. Brasileira Geo.s* 41 4, 566–576.
 Filizola, N., Guyot, J.-L., Beisl, C., Miranda, F.P., 2011. O fluxo de matéria em suspensão na Amazônia ocidental como marcador da dinâmica fluvial. In: De Sousa, W.C., Waichman, A.V., Sinisgalli, P.A., De Angelis, d.A., Romeiro, C.F., Manaus, A.R.E. (Eds.), *Rio Purus: águas, território e sociedade na Amazônia Sul-Occidental.*, (chapter 6).
 Gibbs, R.J., 1967. Amazon River: environmental factors that control its dissolved and suspended load. *Science* 156 (3783), 1734–1737.
 Guyot, J.-L., Filizola, N., Laraque, A., 2005. Régime et bilan du flux sédimentaire de l'Amazone à Óbidos (Pará, Brésil) de 1995 a 2003, *Sediments Budgets* 1, 291. IAHS Publ (347 pp.).
 Latrubesse, E., Stévaux, J., Sinha, R., 2005. Tropical Rivers. *Geomorphology* 70 (3), 187–206.
 Martinez, J.M., Guyot, J.-L., Filizola, N., Sondag, F., 2009. Increase in suspended sediment discharge of the Amazon River assessed by monitoring network and satellite data. *Catena* 79 (3), 257–264.
 Martinez, J.M., Espinoza Villar, R., Armijos, E., Silva Moreira, L., 2015. The optical properties of river and floodplain waters in the Amazon River Basin: implications for satellite-based measurements of suspended particulate matter. *J. Geophys. Res. Earth Surf.* 120 (7), 1274–1287.
 Meade, R.H., Nordin, C.F., Curtis, W.F., Rodrigues, F.M.C., Do Vale, C.M., Edmond, J.M., 1979. Sediment loads in the Amazon River. *Nature* 278, 161–163.
 Meade, R.H., Dunne, T., Richey, J.E., Santos, U., Salati, d.M.E., 1985. Storage and remobilization of suspended sediment in the lower Amazon River of Brazil. *Science* 228 (4698), 488–490.
 Melo, 2012. *Edileuza Carlos de Fatores de controle dos fluxos fluviais de material em suspensão em diferentes cenários climáticos na bacia do Rio Solimões. Tese de Doutorado INPA-UEA, Manaus-Brasil.*
 Mertes, L.A.K., Smith, M.O., Adams, J.B., 1993. Estimating suspended sediment concentrations in surface waters of the Amazon River wetlands from Landsat images. *Remote Sens. Env.* 43 (3), 281–301.
 Mobley, C.D., 1999. Estimation of the remote-sensing reflectance from above-surface measurements. *Appl. Optics* 38, 7442–7455.
 Park, E., Latrubesse, E., 2015. Surface water types and sediment distribution patterns at the confluence of mega rivers: the Solimões-Amazon and Negro Rivers junction. *Water Resour. Res.* 51, 6197–6213.
 Sioli, H., 1984. The Amazon and its main affluents: hydrography, morphology of the river courses and river types. In: *The Amazon*. Springer Netherlands, 127–165.
 Vanoni, V.A., 1977. *Sedimentation Engineering*. ASCE, Am. Soc. Civil Engineers, New York, NY.